Interior Hydroxyls of the Silica Gel System as Studied by ^{29}Si CP–MAS NMR Spectroscopy

I-Ssuer Chuang, David R. Kinney, and Gary E. Maciel*

Contribution from the Department of Chemistry, Colorado State University, Fort Collins, Colorado 80523-0002

Received November 5, 1992

Abstract: Silica gels were deuterium-exchanged with D_2O at 25 and 100 °C. ^{29}Si CP–MAS NMR results indicate that for a silica gel with lower surface area, 9.3% of the single silanols remains undeuterated at 25 °C and 4.0% of the single silanols remains undeuterated at 100 °C. For a higher surface-area silica gel, only 3.0% of the single silanols was not deuterated at 25 °C. In all deuterium-exchanged samples of this study, there is little, if any, evidence of internal geminal silanols. On the basis of the measured T_{Si-H} values and a qualitative study of the ^1H–^{29}Si dipolar interaction strength by an experiment in which the ^1H-decoupling power was varied, it appears that the hydroxyl groups of the internal single silanols undergo rapid rotation about the Si–OH bond axis. ^1H–^1H and ^1H–^{29}Si dipolar dephasing (the former prior to $^1H \rightarrow {}^{29}Si$ cross polarization) indicate that internal single silanols have a much smaller ^1H–^1H dipolar interaction than those experienced by single silanols on the surface and that at least some of the internal single silanols may be accompanied by trapped water.

Introduction

Silicas and modified silicas are highly versatile materials that are used in numerous applications in catalysis, separation science, microelectronics, and composite materials. The widespread utility of silicas is largely a result of their unique surface properties. The most important characteristic of the silica surface, aside from its large size, is the concentration and nature of hydroxyls (silanols) because the surface properties of amorphous silica are largely determined by these characteristics.[1] NMR studies based on ^1H MAS,[2-6] ^1H CRAMPS,[7] ^{29}Si CP–MAS (cross-polarization/magic angle spinning),[4,8-21] and multinuclear strategies,[17-19,22] as well as IR,[4,6,23-45] chemical probes[11-19,23,25,28,29,36-43,46-52] (including deuteration agents[4,6,28,29,33-40,43,44,52-56]), and various other analytical tools[1,4,25,26,57] have been utilized to investigate the nature and/or concentration of hydroxyls on the surface of silicas. Among the chemical strategies that have been used to characterize silica is deuterium exchange by reaction with deuterium oxide, which, for surface hydroxyls, is complete after several cycles of exchange

(1) Iler, R. K. *The Chemistry of Silica*; Wiley: New York, 1979.
(2) Freude, D.; Hunger, M.; Pfeifer, H. *Chem. Phys. Lett.* **1982**, *91*, 307.
(3) Hunger, M.; Freude, D.; Pfeifer, H.; Bremer, H.; Jank, M.; Wendlandt, K.-P. *Chem. Phys. Lett.* **1983**, *100*, 29.
(4) Köhler, J.; Chase, D.; B.; Farlee, R. D.; Vega, A. J.; Kirkland, J. J. *J. Chromatogr.* **1985**, *352*, 275.
(5) Pfeifer, H.; Freude, D.; Hunger, M. *Zeolites* **1985**, *5*, 274.
(6) Davydov, V. Y.; Kiselev, A. V.; Pfeifer, H.; Junger, I. *Russ. J. Phys. Chem.* **1983**, *57*, 1527.
(7) Bronnimann, C. E.; Zeigler, R. C.; Maciel, G. E. *J. Am. Chem. Soc.* **1988**, *110*, 2023.
(8) Maciel, G. E.; Sindorf, D. W. *J. Am. Chem. Soc.* **1980**, *102*, 7606.
(9) Sindorf, D. W.; Maciel, G. E. *J. Am. Chem. Soc.* **1983**, *105*, 1487.
(10) Maciel, G. E.; Sindorf, D. W.; Bartuska, V. J. *J. Chromatogr.* **1981**, *205*, 438.
(11) Sindorf, D. W.; Maciel, G. E. *J. Am. Chem. Soc.* **1981**, *103*, 4263.
(12) Sindorf, D. W.; Maciel, G. E. *J. Phys. Chem.* **1982**, *86*, 5208.
(13) Sindorf, D. W.; Maciel, G. E. *J. Am. Chem. Soc.* **1983**, *105*, 3767.
(14) Sindorf, D. W.; Maciel, G. E. *J. Phys. Chem.* **1983**, *87*, 5516.
(15) Claessens, H. A.; de Haan, J. W.; Van de Ven, L. J. M.; de Bruyn, P. C.; Cramers, C. A. *J. Chromatogr.* **1988**, *436*, 345.
(16) Pfleiderer, B.; Albert, K.; Bayer, E.; Van de Ven, L.; de Haan, J.; Cramers, C. *J. Phys. Chem.* **1990**, *94*, 4189.
(17) Caravajal, G. S.; Leyden, D. E.; Quinting, G. R.; Maciel, G. E. *Anal. Chem.* **1988**, *60*, 1776.
(18) Maciel, G. E.; Bronnimann, C. E.; Zeigler, R. C.; Chuang, I-S.; Kinney, D. R.; Keiter, E. A. In *The Colloid Chemistry of Silica*; Bergna, H., Ed.; Advances in Chemistry Series 234; American Chemical Society: Washington, DC, in press.
(19) Akapo, S. O.; Simpson, C. F. *J. Chromatogr. Sci.* **1990**, *28*, 186.
(20) Morrow, B. A.; Gay, I. D. *J. Phys. Chem.* **1988**, *92*, 5569.
(21) Chuang, I-S.; Kinney, D. R.; Bronnimann, C. E.; Zeigler, R. C.; Maciel, G. E. *J. Phys. Chem.* **1992**, *96*, 4027.
(22) Bernstein, T.; Kitaev, L.; Michel, D.; Pfeifer, H.; Fink, P. *J. Chem. Soc., Faraday Trans. 1* **1982**, *78*, 761.
(23) Synder, L. R.; Ward, J. W. *J. Phys. Chem.* **1966**, *70*, 3941.
(24) Peri, J. B. *J. Phys. Chem.* **1966**, *70*, 2937.
(25) Hair, M. L. *Infrared Spectroscopy in Surface Chemistry*; Marcel Dekker: New York, 1967.
(26) Mikhail, R. S.; Robens, E. *Microstructure and Thermal Analysis of Solid Surfaces*; John Wiley & Sons: New York, 1983.
(27) Kondo, S.; Yamauchi, H.; Kajiyama, Y.; Ishikava, T. *J. Chem. Soc., Faraday Trans. 1* **1984**, *80*, 2033.
(28) Morrow, B. A.; McFarlan, A. J. *J. Non-Cryst. Solids* **1990**, *120*, 61.
(29) Van Roosmalen, A. J.; Mol, J. C. *J. Phys. Chem.* **1978**, *82*, 2748.
(30) Morrow, B. A.; McFarlan, A. J. *J. Phys. Chem.* **1992**, *96*, 1395.
(31) McFarlan, A. J.; Morrow, B. A. *J. Phys. Chem.* **1991**, *95*, 5388.
(32) Hoffmann, P.; Knözinger, E. *Surf. Sci.* **1987**, *188*, 181.
(33) Hambleton, F. H.; Hockey, J. A.; Taylor, J. A. G. *Trans. Faraday Soc.* **1966**, *62*, 801.
(34) Hambleton, F. H.; Hockey, J. A.; Taylor, J. A. G. *Nature* **1965**, *208*, 138.
(35) Davydov, V. Y.; Kiselev, A. V. *Russ. J. Phys. Chem.* **1963**, *37*, 1404.
(36) Davydov, V. Y.; Kiselev, A. V.; Zhuravlev, L. T. *Trans. Faraday Soc.* **1964**, *60*, 2254.
(37) Kiselev, A. V. *Discuss. Faraday Soc.* **1971**, *52*, 14.
(38) Burneau, A.; Barrès, O.; Gallas, J. P.; Lavalley, J. C. *Langmuir* **1990**, *6*, 1364.
(39) Gallas, J. P.; Lavalley, J. C.; Burneau, A.; Barrès, O. *Langmuir* **1991**, *7*, 1235.
(40) Morrow, B. A.; McFarlan, A. J. *Langmuir* **1991**, *7*, 1695.
(41) Armistead, C. G.; Tyler, A. J. Hambleton, F. H.; Mitchell, S. A.; Hockey, J. A. *J. Phys. Chem.* **1969**, *73*, 3947.
(42) Tripp, C. P.; Hair, M. L. *Langmuir* **1991**, *7*, 923.
(43) Davydov, V. Y.; Kiselev, A. V.; Lokutsievskii, V. A.; Lygin, V. I. *Russ. J. Phys. Chem.* **1973**, *47*, 460.
(44) Benesi, H. A.; Jones, A. C. *J. Phys. Chem.* **1959**, *63*, 179.
(45) McDonald, R. S. *J. Phys. Chem.* **1958**, *62*, 1168.
(46) Peterson, E. M.; O'Reilly, D. E.; Tsang, T. *J. Chem. Phys.* **1979**, *70*, 3409.
(47) Yamauchi, H.; Kondo, S. *Colloid Polym. Sci.* **1988**, *266*, 855.
(48) Machin, W. D.; Golding, P. D. *J. Chem. Soc., Faraday Trans. 1* **1990**, *86*, 171, 175.
(49) Kellum, G. E.; Smith, R. C.; Uglum, K. L. *Anal. Chem.* **1968**, *40*, 2058.
(50) Morrow, B. A.; McFarlane, R. A. *J. Phys. Chem.* **1986**, *90*, 3192.
(51) Fripiat, J. J.; Uytterhoeven, J. *J. Phys. Chem.* **1962**, *66*, 800.
(52) Mathias, J.; Wannemacher, G. *J. Colloid Interface Sci.* **1988**, *125*, 61.
(53) Zhuravlev, L. T. *Langmuir* **1987**, *3*, 316 and references therein.
(54) Fripiat, J. J.; Gastuche, M. C.; Brichard, R. *J. Phys. Chem.* **1962**, *66*, 805.
(55) Zhuravlev, L. T.; Kiselev, A. V.; Naidina, V. P.; Polyakov, A. L. *Russ. J. Phys. Chem.* **1963**, *37*, 1113.
(56) Zhuravlev, L. T.; Kiselev, A. V.; Naidina, V. P.; Polyakov, A. L. *Russ. J. Phys. Chem.* **1963**, *37*, 1216.
(57) Cooney, R. P.; Curthoys, G.; Tam, N. T. *Adv. Catal.* **1975**, *24*, 293.

0002-7863/93/1515-8695$04.00/0

at room temperature[6,24,35-37,40,43] (except for those silicas that have experienced prior treatment at high temperature, e.g., 600 °C[29]). IR studies of silicas after deuterium exchange have revealed that an absorption band around 3660 cm^{-1} is not affected by deuterium; this band is assigned to hydroxyl groups buried in the bulk and inaccessible for deuterium exchange, i.e., *internal* silanols.[6,33-40] Hambleton et al.[33] confirmed that the 3650-cm^{-1} IR band belongs to weakly interacting hydroxyls sited on neighboring silicon atoms *within* the solid lattice of the silica particles. Davydov and co-workers investigated deuterated silicas in the IR overtone region and also concluded that the IR fundamental band at 3650 cm^{-1} belongs to internal silanol hydroxyls.[37,43]

This article describes the utilization of ^{29}Si CP–MAS NMR techniques to determine the amounts and nature of internal silanols in two silicas with different surface areas. If not well understood, the effects of these internal silanols can complicate interpretations in ^{29}Si CP–MAS NMR studies of external silanols. With a greater knowledge of the properties of these internal silanols, one can hope to ultimately improve the interpretation of ^{29}Si CP–MAS studies and the understanding of external silanols.

Experimental Section

The silica gels used in this study (Fisher Scientific S-679) are high-purity, high surface-area silicas prepared by precipitation from sodium silicate solutions. Slight changes in the manufacturer's preparation of the silica resulted in the availability of two different materials that we will call "higher surface-area" (HSA) and "lower surface-area" (LSA) silicas. Characteristics of these silicas provided by the manufacturer (Davison Chemical Division, W.R. Grace & Co.) include the following: particle size distribution ranging from 75 to 150 μm, N_2/BET-determined surface areas of 666 m^2/g for the HSA gel (lot no. 744553) and 422 m^2/g for the LSA gel (lot no. 740341), and average pore-size distributions of 26 and 30 Å, respectively. The samples referred to as being "untreated" HSA or LSA silicas were simply used as received from the supplier.

Two slightly different procedures were employed to bring about deuterium exchange of silica gel at 25 °C. In one procedure, 3.0 g of untreated silica gel was mixed with 10 mL of 99.9% deuterium oxide (Isotec, Inc.) under air in a closed flask at 25 °C with constant stirring. After 15 min, the supernatant liquid was poured out and the same procedure was repeated for a total of eight exchanges. The resulting, wet silica gel was evacuated under a vacuum of 10^{-2} Torr over the course of 2 h. A second procedure that was also used was intended to minimize residual protons on the silica surface due to exchange of the D_2O-exchanged surface with ^1H_2O in air. For this procedure, 5 g of untreated silica gel was loaded into a flask that had an attached addition funnel filled with D_2O. The flask was sealed, and 12 mL of the D_2O was added to the silica gel with stirring. The liquid D_2O was gradually evaporated under a vacuum at 25 °C over the next 1–2 h. Once the silica gel had dried enough to flow freely as a powder, a second 12-mL aliquot of D_2O was added at a pressure less than ambient. The procedure was repeated for a total of four exchanges without ever opening the flask to air. After the final exchange, the sample was dried under a vacuum of 10^{-3} Torr at 25 °C with stirring for 12 h. The ^{29}Si CP–MAS NMR spectra showed no difference between samples prepared by the two procedures described above. Deuterium-exchanged silicas prepared using either of these two methods are designated as HSA-*d*-25 and LSA-*d*-25 (for the higher surface-area and lower surface-area gels, respectively) in the discussion below. A "control" silica gel sample was prepared according to the second procedure described above with only one exception; distilled ^1H_2O was used instead of 99.9% D_2O. This sample was prepared using LSA silica and is designated as LSA-^{1}H-25. In all D_2O-exchange procedures, all glassware had been rinsed with D_2O before use. The purity of the D_2O was confirmed by ^1H NMR, using the method of standard additions.

After investigation by ^{29}Si CP–MAS, LSA-*d*-25 was exposed to air with stirring for 90 s, 3 min, 10 min, 30 min, 90 min, and 15 days. After exchanging with ^1H_2O in air, these samples incorporated increasing concentrations of protons into their surface silanols, as will be seen in the Results and Discussion section below. After sample HSA-*d*-25 was studied by NMR, it was exchanged with a 95% D_2O/5% H_2O solution. The exchange was performed a total of eight times in air. The resulting, wet silica was then evacuated at 10^{-2} Torr and 25 °C over the course of 2 h. This sample is referred to as HSA-95*d*-25.

LSA silica was also deuterium-exchanged under reflux conditions. A 10-g sample of LSA silica was sealed in a flask with 12 mL of D_2O and additional D_2O in an attached addition funnel. After the D_2O/silica mixture was allowed to reflux under dry N_2 for 24 h, the flask was cooled to 25 °C and the D_2O was evaporated under a vacuum of 10^{-3} Torr over the next 1–2 h. Once the silica had dried enough to flow freely as a powder, another 12-mL aliquot was added to the silica and the procedure was repeated. A total of four reflux exchanges were performed, after which a fifth exchange was performed at 25 °C. The final 25 °C exchange avoided the need for nitrogen as an inert gas and eliminated the possibility of surface protonation by any residual water in the dry N_2(g). This sample is referred to as LSA-*d*-100.

Another LSA sample was prepared by evacuating the silica at high temperature. A 4.5-g sample of untreated LSA silica was loaded into a ceramic boat at a depth of 1 cm and evacuated under a vacuum of 10^{-3} Torr for 2 h. The temperature was then increased at a rate of 2 °C/min to a final temperature of 500 °C. The silica was evacuated at 500 °C for 9 h and then allowed to cool to room temperature. This sample is referred to as LSA-500.

Samples studied by ^{29}Si NMR were loaded into a 2.5 cm^3 Pencil MAS rotor (provided by Chemagnetics, Inc.) with a zirconia sleeve and a tightly fitted press-fit cap. The deuterium-exchanged samples were loaded into rotors that had been rinsed with 99.9% D_2O and evacuated at 10^{-2} Torr and 25 °C for 3 h. All sample transfers took place under a dry nitrogen atmosphere in a glovebox. A LSA-*d*-25 silica sample was subjected to magic-angle spinning with air as the driving gas. No change was observed in the ^{29}Si CP–MAS spectra of the deuterium-exchanged samples over the course of 3 days. However, over a 10-day period, some changes were observed. Hence, the ^{29}Si CP–MAS spectra of all other deuterium-exchanged samples were obtained with dry nitrogen as the MAS drive gas as a precaution. Samples that were analyzed by ^1H NMR were loaded into 5-mm o.d. thin-wall glass NMR tubes under dry nitrogen. The tubes were flame-sealed under N_2(g) at a pressure of 0.5 atm.

^{29}Si NMR spectra were obtained on a heavily modified NT-200 spectrometer (with a ^{29}Si Larmor frequency of 39.75 MHz) under ^1H–^{29}Si cross-polarization[58] and magic-angle spinning conditions.[59-61] In most cases, high-power ^1H decoupling was employed. Measurements of the proton spin–lattice relaxation time (T_1^H) were made by detecting the ^{29}Si CP–MAS intensity that was cross-polarized from the protons, according to a Freeman–Hill version of a CP–MAS T_1^H experiment.[62] Proton spin–lattice relaxation times ($T_{1\rho}^H$) in the rotating frame of the applied radiofrequency field were measured independently of $^1H \rightarrow {}^{29}Si$ cross-polarization dynamics by varying the duration of a ^1H spin–lock period prior to a fixed $^1H \rightarrow {}^{29}Si$ cross-polarization contact period. The cross-polarization contact time in this experiment was 1 ms for proton-bearing silicas and 20 ms for deuterium-exchanged silicas. The cross-polarization time constants (T_{Si-H}) were determined by analysis of variable contact-time experiments, using the independently-determined $T_{1\rho}^H$ values in a nonlinear least-squares fit of the variable contact-time data. Other parameters and pulse sequences used are shown in the Results and Discussion section. The MAS rate was kept constant at 1.6 kHz. ^{29}Si NMR chemical shifts (in ppm) were referenced to liquid tetramethylsilane (by substitution), a higher shift corresponding to lower shielding.

Proton combined rotation and multiple pulse spectroscopy (CRAMPS) experiments were performed at 187 MHz on a severely modified Nicolet NT-200 spectrometer.[63] The BR-24 pulse sequence[64] was used with a $\pi/2$ pulse length of 1.3 μs and a pulse spacing of 3 μs. Sealed samples were spun at 1.0 kHz, using a spinner corresponding to the design of Gay.[65] Chemical shifts were determined by external referencing via substitution of samples containing tetrakis(trimethylsilyl)methane and are reported here relative to tetramethylsilane.

Results and Discussion

The HSA and LSA silicas were examined using ^{29}Si CP–MAS and ^1H CRAMPS NMR prior to deuterium exchange. Figures 1a and 1b show the ^{29}Si CP–MAS spectra of untreated HSA and

(58) Pines, A.; Gibby, M. G.; Waugh, J. S. *J. Chem. Phys.* **1973**, *59*, 569.
(59) Andrew, E. R. *Prog. NMR Spectrosc.* **1971**, *8*, 1.
(60) Lowe, I. J. *Phys. Rev. Lett.* **1959**, *2*, 285.
(61) Schaefer, J.; Stejskal, E. *J. Am. Chem. Soc.* **1976**, *98*, 1031.
(62) Frye, J. S. *Concepts Magn. Reson.* **1989**, *1*, 27.
(63) Bronnimann, C. E.; Hawkins, B. L.; Zhang, M.; Maciel, G. E. *Anal. Chem.* **1988**, *60*, 1743.
(64) Burum, D. P.; Rhim, W. K. *J. Chem. Phys.* **1979**, *71*, 944.
(65) Gay, I. D. *J. Magn. Reson.* **1984**, *58*, 413.

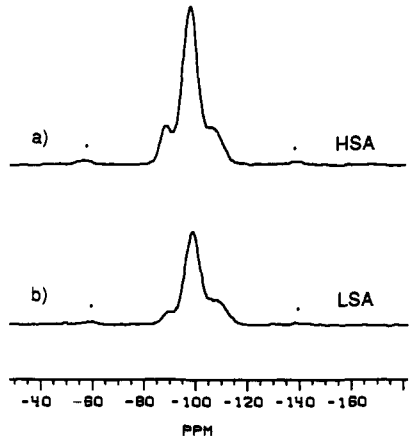

Figure 1. 39.75-MHz ^{29}Si CP–MAS NMR spectra of two untreated silica gel samples plotted on the same intensity scale. Asterisks indicate MAS sidebands; CP contact time = 1 ms; repetition delay = 0.6 s; 200 scans: (a) HSA silica and (b) LSA silica.

Table I. Relaxation Time Constants for Various Silicas, as Determined by ^{29}Si CP–MAS at 39.75 MHz

	T_{Si-H} (ms)[a]		$T_{1\rho}^{H}$ (ms)[b]		T_1^H (s)[c]	
sample	−99 ppm	−109 ppm	−99 ppm	−109 ppm	−99 ppm	−109 ppm
HSA	2.5	16.8	36	37	0.22	0.24
LSA	2.1	17.0	11	12	0.26	0.26
LSA-^{1}H-25	2.5	14.0	33	33	0.29	0.31
HSA-*d*-25	12.7	24.9	115	122	6.0	6.7
LSA-*d*-25	11.4	19.2	110	110	6.8	6.8
LSA-*d*-100	11.4	19.2	110	110	6.2	6.8

[a] Estimated errors: ±10%. [b] Estimated errors: ±10%. [c] Estimated errors: ±5%.

LSA, respectively. The spectra illustrate the well-established basic features seen in ^{29}Si NMR spectra of amorphous silicas.[4,8-21] The peak at −89 ppm is attributed to silicon atoms that have two geminal hydroxyl groups attached, $(\equiv SiO)_2Si(OH)_2$, often referred to as Q_2 silicons. The resonance at −99 ppm is due to silicons with only one hydroxyl group, $(\equiv SiO)_3SiOH$ (Q_3). Any siloxanes, $Si(OSi\equiv)_4$ (Q_4), that can be cross-polarized by nearby protons give rise to the peak at −109 ppm. The small peaks indicated by asterisks in the figures are spinning sidebands.

As the vast majority of protons in untreated silica particles are on the surface, the ^{1}H → ^{29}Si CP ^{29}Si NMR spectra of these materials are dominated by surface silicons. The higher intensity seen in Figure 1 for the HSA silica compared to that for the LSA silica illustrates the capability of ^{29}Si CP–MAS to reflect the difference in surface area between the two samples. In order to quantitate the ratio of surface areas using CP–MAS NMR, one must consider the relevant cross-polarization relaxation parameters ($T_{1\rho}^H$ and T_{Si-H}) and spin–lattice relaxation constants (T_1^H) measured for each sample and compiled in Table I. After compensation for differences in CP and spin–lattice relaxation dynamics, the overall integrated ^{29}Si CP–MAS intensity of the HSA silica was found to be 1.6 times greater than that of the LSA silica. This factor accurately reflects the ratio of nitrogen BET surface areas of the two samples. This ratio of ^{29}Si CP–MAS intensities was found in spectra obtained with 5- and 20-ms CP contact times as well as the 1-ms contact-time spectra shown in Figure 1. Aside from the overall relative spectral intensities, the only other difference found in the ^{29}Si CP–MAS spectra of HSA and LSA silicas in Figure 1 is the slightly lower fraction of geminal (Q_2) silanols seen for the LSA silica. This may reflect structural differences that give rise to the measured difference in surface areas of these two silica gels. Aside from differences in CP dynamics that will be discussed below, the spectrum of

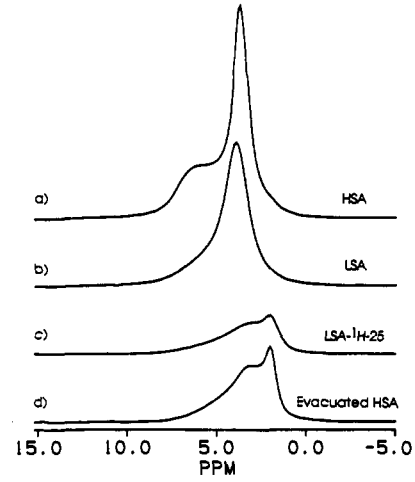

Figure 2. 187.1-MHz ^{1}H CRAMPS spectra of various silicas obtained in 100 scans, using a 5-s recycle delay. Spectra are plotted using the same intensity scale after compensation for small differences in the mass of each sample, which was approximately 0.1 g: (a) HSA silica; (b) LSA silica; (c) LSA-^{1}H-25 silica, and (d) HSA silica that was evacuated to 10^{-3} Torr at 25 °C until 4.1% of the initial sample weight was removed.

LSA-^{1}H-25 silica (see Figure 4c) is virtually identical to that of untreated LSA silica.

^{1}H CRAMPS spectra of the untreated HSA and LSA silicas are shown in Figures 2a and 2b, respectively. Both spectra illustrate features that have been previously assigned.[7] The tall peak centered at approximately 4 ppm is due to physisorbed water. The broad component ranging from about 2 to 8 ppm is attributed to silanol protons in various hydrogen-bonding environments and very strongly hydrogen-bonded (relatively rigid) water. The integrated ^{1}H CRAMPS intensity of the HSA silicon spectrum is 1.2 times greater than that of the LSA silica; this factor does not reflect the surface-area ratio of these samples because the ^{1}H CRAMPS experiment measures signals due to both silanol protons and protons of adsorbed water. As seen in the spectra, the untreated LSA silica has a larger ratio of physisorbed water to silanols than the HSA silica. Figure 2c shows that the LSA-^{1}H-25 silica is drier than either untreated sample; very little physisorbed water intensity is observed at 4 ppm. As a result of not being dominated by the physisorbed water peak, the spectrum of LSA-^{1}H-25 shows an additional feature, a peak at 1.8 ppm, which is assigned to silanol protons that are not involved in hydrogen bonding. This peak typically becomes visible as silicas are dehydrated,[7] and its appearance in Figure 2c merely reflects the fact that LSA-^{1}H-25 is drier than the untreated silicas. When a sample of HSA silica was dried under vacuum at 25 °C to the same extent as the LSA-^{1}H-25 silica (as indicated by the intensity of the water peak relative to the isolated silanol peak), the ^{1}H CRAMPS spectrum (Figure 2d) exhibits the same features seen in the spectrum of the LSA-^{1}H-25 silica. Without the interference of variable amounts of physisorbed water, integration of the spectra in Figures 2c and 2d reveals that the ^{1}H CRAMPS silanol intensity also accurately reflects the surface area ratio of 1.6 for these two silicas.

The ^{29}Si CP–MAS spin dynamics of the silicas also reflect the differences in hydration between untreated (LSA) and LSA-^{1}H-25 samples. As shown in Table I, T_1^H of the drier LSA-^{1}H-25 silica is only slightly larger than that of the untreated LSA silica. However, $T_{1\rho}^H$ is much smaller (12 ms) for the wetter LSA silica than for the drier LSA-^{1}H-25 silica (33 ms). The effects of rotating-frame proton relaxation on the ^{29}Si CP–MAS spectra can be seen in Figure 3. While the intensities of the silanol peaks at −89 and −99 ppm for the LSA silica are seen to diminish when the CP contact time is increased from 5 to 20 ms (Figures 3b and 3c, respectively), the same peaks in the 20-ms contact-time spectrum of LSA-^{1}H-25 silica (Figure 3f) have virtually the same

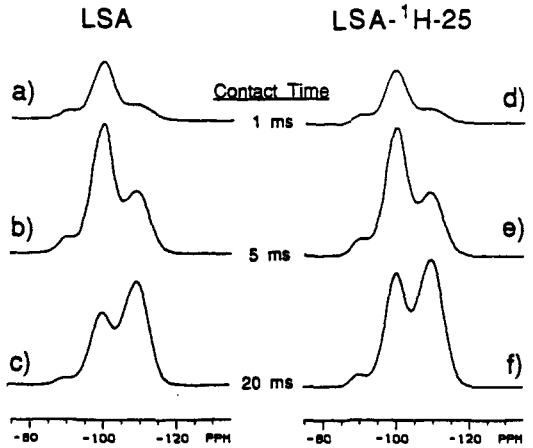

Figure 3. 39.75-MHz ^{29}Si CP–MAS NMR spectra of LSA silica and LSA-^{1}H-25 silica with three different CP contact times. The spectra of a given sample were all plotted on the same intensity scale. Repetition delay = 1 s; 1000 scans. For LSA silica, contact time is (a) 1 ms, (b) 5 ms, and (c) 20 ms; for LSA-^{1}H-25, contact time is (d) 1 ms, (e) 5 ms, and (f) 20 ms.

intensities as those observed with a 5-ms contact time (Figure 3e). The effects of $T_{1\rho}^H$ relaxation on the relative intensities within the spectra of the drier LSA-^{1}H-25 are much less severe than those seen for the untreated silica.

The spectra in Figure 3 appear to show no evidence of $T_{1\rho}^H$ relaxation effects on the –109 ppm siloxane peaks. As there is strong evidence of $T_{1\rho}^H$ relaxation effects on the silanol peaks in Figures 3b and 3c, this might lead one to believe that the external siloxanes have a different proton source of cross polarization that has a larger $T_{1\rho}^H$ value than that of the proton polarization source for the external silanols of the untreated LSA silica. However, more careful analysis of the variable contact-time results, in conjunction with independently-measured $T_{1\rho}^H$ values (*vide infra*), reveals that both the external siloxane and external silanol magnetizations decay at a rate determined by a *common* $T_{1\rho}^H$ value. Nevertheless, as expected, the siloxane peak has a much larger T_{Si-H} value than the silanol peak. The slow growth of external siloxane CP intensity as the contact time is increased obscures the observation of $T_{1\rho}^H$ decay that is so evident for the external silanol peaks (which have much smaller T_{Si-H} values) in the same variable contact-time spectra (shown in Figures 3a–c for the LSA silica). Since the external silanol and external siloxane peaks have common $T_{1\rho}^H$ and T_1^H values, we conclude that both share the same (silanol) proton spin reservoir as a source of $^1H \rightarrow {}^{29}Si$ cross polarization.

Figure 4 displays ^{29}Si CP–MAS NMR spectra of untreated LSA, LSA-^{1}H-25, LSA-*d*-25, and LSA-*d*-100 silicas. The ^{29}Si NMR intensity is clearly depleted dramatically in the D_2O-exchanged samples (Figures 4b and 4d), reflecting the loss of most of the proton reservoir for $^1H \rightarrow {}^{29}Si$ cross polarization. In order to quantify the extent of deuterium exchange in the two samples, T_1^H and cross-polarization dynamics of the ^{29}Si CP–MAS experiment for each sample must be considered. A single, common T_1^H value is observed to dominate the spin–lattice relaxation of all peaks within each spectrum of Figure 4. These T_1^H values are 0.26 s for untreated LSA, 0.30 s for LSA-^{1}H-25, and 6.8 s for the two D_2O-exchanged samples. Figure 5 illustrates variable contact-time behavior for LSA-^{1}H-25 and LSA-*d*-25. The large T_{Si-H} value of the siloxane peak of the LSA-^{1}H-25 silica once again obscures the fact that both the silanol and siloxane peaks of this sample exhibit a common $T_{1\rho}^H$ value. Both peaks of the D_2O-exchanged silica do in fact exhibit larger $T_{1\rho}^H$ *and* larger T_{Si-H} values than those seen for the corresponding proton-rich silica. The relevant time constants are also tabulated in Table I. After correcting for relaxation behavior in terms of the

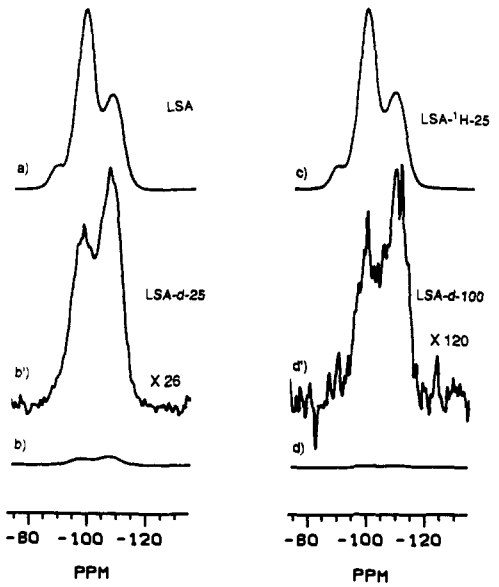

Figure 4. 39.75-MHz ^{29}Si CP–MAS NMR spectra of four different silicas. Contact time = 5 ms: (a) untreated LSA with a 0.6-s repetition delay and 5256 scans; (b and b′) LSA-*d*-25 with a 10-s repetition delay and 5256 scans, (b) plotted on the same intensity scale as used in plot (a) and (b′) at 26-times this intensity scale; (c) LSA-^{1}H-25 with a 0.6-s repetition delay and 8000 scans; and (d and d′) LSA-*d*-100 with a 3-s repetition delay and 8000 scans, (d) plotted on the same intensity scale as used in plot (c) and (d′) at 120-times this intensity scale.

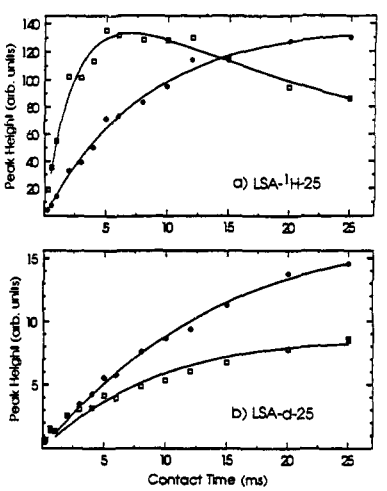

Figure 5. 39.75-MHz variable contact-time ^{29}Si CP–MAS results for (a) LSA-^{1}H-25 silica and (b) LSA-*d*-25; (□) for –99 ppm single-silanol peak and (•) for –109 ppm siloxane peak.

measured parameters ($T_{1\rho}^H$, T_1^H, and T_{Si-H}), we determined the amount of proton-bearing single silanol (–99 ppm) remaining in the D_2OH-exchanged sample LSA-*d*-25 to be 9.3% of the single silanols in the ^1H_2O-exchanged sample LSA-^{1}H-25. The sample that was D_2O-exchanged at 100 °C (LSA-*d*-100) contains only 4.0% of the amount of proton-bearing single silanols seen in the control sample LSA-^{1}H-25.

The ^{29}Si CP–MAS spectra of untreated HSA silica and HSA-*d*-25 silica are shown in Figure 6. The relative intensities of the various peaks within each spectrum are very similar to those seen for the analogous LSA samples. After accounting for differences in relaxation parameters and the number of scans, one can calculate that only 3.0% of the single silanols in the HSA-*d*-25 silica remain proton-bearing.

In order to establish any relationship or contrast the differences between the small population of unexchangeable protons in these silicas and the majority of exchangeable protons, the D_2O-exchanged samples were partially ^1H_2O exchanged, using the

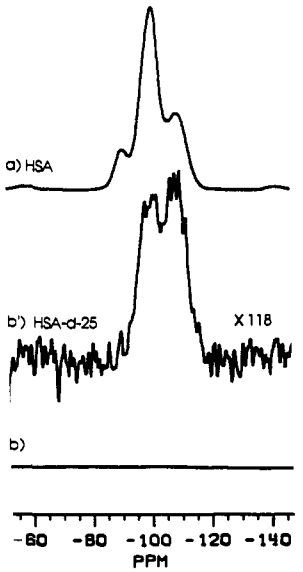

Figure 6. 39.75-MHz ^{29}Si CP–MAS NMR spectra of two HSA silicas. Contact time = 5 ms: (a) untreated HSA with a 0.6-s repetition delay and 5256 scans and (b and b′) HSA-*d*-25 with a 3-s repetition delay and 9650 scans, (b) plotted at the same intensity scale as used in plot (a) and (b′) at 118-times this intensity scale.

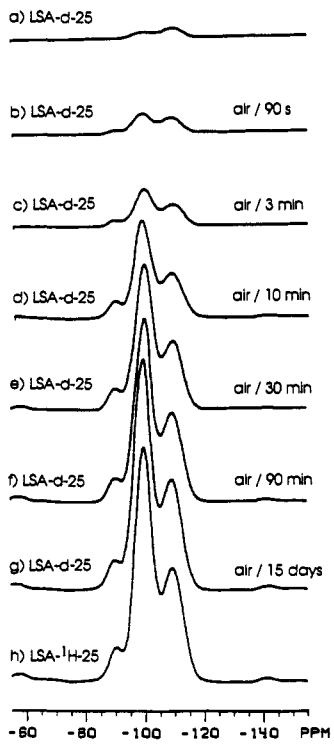

Figure 7. 39.75-MHz ^{29}Si CP–MAS NMR spectra of LSA at eight different deuteration levels. Contact time = 5 ms; 11 088 scans: (a) LSA-*d*-25, (b) LSA-*d*-25 exposed to air for 90 s, (c) LSA-*d*-25 exposed to air for 3 min, (d) LSA-*d*-25 exposed to air for 10 min, (e) LSA-*d*-25 exposed to air for 30 min, (f) LSA-*d*-25 exposed to air for 90 min, (g) LSA-*d*-25 exposed to air for 15 days, and (h) LSA-^{1}H-25. All spectra are plotted on the same intensity scale. Repetition time = 3 s for (a)–(e) and 1 s (f)–(h).

two methods described in the Experimental Section. The ^{29}Si CP–MAS spectra of the LSA silica at various proton population levels are shown in Figure 7. Figure 7b is the spectrum of the LSA-*d*-25 silica after exposure to isotopically normal water in air for only 90 s. By comparing the intensity of this spectrum to that of the original unexposed LSA-*d*-25 silica in Figure 7a, we can see that very few silanol sites have been reprotonated during the brief air exposure, presumably exterior silanols.

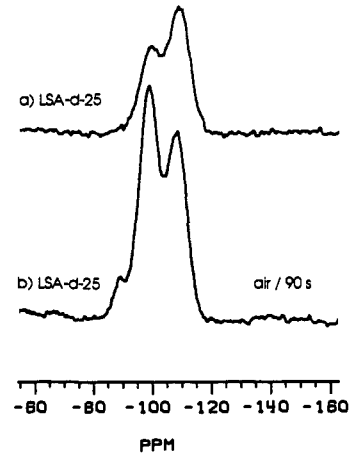

Figure 8. Vertically expanded versions of Figures 7a and 7b: (a) Figure 7a expanded ×10 and (b) Figure 7b expanded ×10.

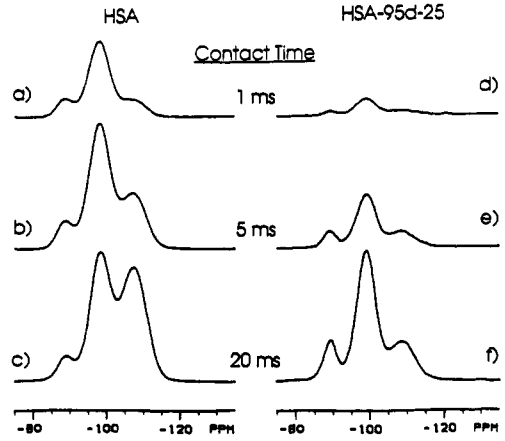

Figure 9. 39.75-MHz ^{29}Si CP–MAS NMR spectra of HSA and HSA-95*d*-25 with three different contact times. For a given sample, all the spectra are plotted on the same intensity scale. For HSA silica, repetition delay = 0.6 s; 1000 scans; contact time is (a) 1 ms, (b) 5 ms, and (c) 20 ms. For HSA-95*d*-25, repetition delay = 1 s; 5256 scans; contact time is (d) 1 ms, (e) 5 ms, and (f) 20 ms.

However, even at this very low level of *exterior* proton population, the line shape of the ^{29}Si CP–MAS spectrum has changed dramatically. While the LSA-*d*-25 spectrum in Figure 7a, even in a vertically expanded form (Figure 8a), shows very little, if any, evidence of proton-bearing geminal silanols, the spectrum of the partially reprotonated silica in Figures 7b and 8b clearly shows evidence of the presence of geminal silanols at –89 ppm in nearly the same relative concentration seen at all higher protonation levels. Another distinctive feature of the (partially) reprotonated silicas is the higher intensity of the –99 ppm single-silanol peak relative to that of the –109 ppm siloxane peak, in comparison to what is seen in the spectra of D_2O-exchanged material (compare Figures 7a/8a with Figures 7b–h). In all of the spectra of D_2O-exchanged silicas, the siloxane peak intensity is greater than the single-silanol peak intensity.

Figure 9 compares spectra of untreated HSA with the ^{29}Si CP–MAS spectra, obtained using various CP contact times, of a sample of HSA-*d*-25 silica that was reprotonated through exchange with a 95% D_2O/5% H_2O solution (HSA-95*d*-25). The relatively low level of proton population in the partially reprotonated sample generates geminal silanol intensity at –89 ppm and increases the peak intensity of the single silanols relative to that of the siloxanes (as compared to the HSA-*d*-25 spectrum of Figure 6b′). In the spectra of untreated HSA silica in Figures 9a–c, increasing the CP contact time from 1 to 20 ms results in only modest increases in single and geminal silanol intensities. However, the variable contact-time results in Figures 9d–f for

the HSA-95*d*-25 silica indicate that most of the silanols of this silica have much larger cross-polarization time constants (T_{Si-H} = 12.7 ms) than the 2.5-ms value measured for the untreated HSA silica. The intensities of the silanol peaks in the spectra of the HSA-95*d*-25 silica exhibit substantial growth in going from a 5- to a 20-ms contact time. This decrease in the cross-polarization rate constant for this partially proton-bearing silica, relative to that of the untreated silica, is likely due to the lack of protons on the majority of the silanol groups on the surface of this silica; the predominant $(-O-)_3SiOD$ and $(-O-)_2Si(OD)_2$ silicons must depend on the 5% of nearby proton-bearing silanols for polarization via CP. As the internuclear distance between the majority of deuterium-bearing silanol ^{29}Si nuclei and the nearest proton on a rare, neighboring, proton-bearing silanol is inevitably greater than the distance between a proton-bearing silanol ^{29}Si nucleus and its hydroxyl proton, the $^1H-^{29}Si$ dipolar interaction for this majority of deuterium-bearing silanols will be accordingly weaker. As cross polarization depends upon this heteronuclear dipolar interaction, the greater distance is manifested in larger cross-polarization time constants (T_{Si-H}). The spin dynamics of silicas with various known levels of surface deuterium exchange are currently being studied in order to obtain information on the kind(s) and number of nearest neighbors to these single and geminal silanols.

The D_2O exchange of these silicas has clearly revealed that a portion of the silanols is highly resistant to deuterium exchange. The experimental evidence also provides many indications that the unexchanged protons are unlike the majority of exterior protons of untreated silica gel and that these unexchanged protons may be silanol and water protons that are trapped inside the bulk structure of silica particles. It is highly unlikely that the unexchanged protons are residual exterior protons. Several previous studies have proven that exterior protons of silicas undergo rapid D_2O exchange.[6,24,35-37,40,43] The rapid $^2D-^1H$ exchange seen in the results shown in Figure 7 indicates that the exterior silanol protons exchange rapidly, even with water vapor in air. Careful and thorough exchanges with 99.9% *liquid* D_2O would be expected to leave, at most, only a few tenths of a percent of unexchanged exterior protons, not the 3.0–9.3% observed here. The fact that performing the D_2O exchange at elevated temperatures significantly increases the level of deuterium exchange suggests that many of these less accessible (ostensibly *internal*) protons may be accessible from the exterior through highly restricted micropores or fissures on the surfaces of silica particles. The steric aspects of reprotonation by $R-O-^1H$ species of various sizes may provide information on the micropores and fissures in these systems; such studies are underway.

For the HSA and LSA silicas, comparing the percentages of protons that are unexchanged by D_2O also provides insight into the structure of these materials. Analytical data supplied by the manufacturer of the silicas indicate that the surface area of the HSA silica is larger, while the particle size is the same as that of the LSA silica, because of a smaller average pore diameter in the HSA silica. A larger number of small pores rather than large pores can be accommodated on a particle of a given diameter. The result is an HSA particle with more of its internal volume penetrated by smaller and more numerous pores; this leaves less internal volume for trapped or unexchangeable protons. Of course, one should recognize that surface areas measured by the BET-(N_2) method may not give an accurate assessment of the accessibility of H_2O to the surface. Nevertheless, our NMR data for the D_2O exchange at 25 °C support this structural feature. The LSA silica has 3.1 times more unexchangeable protons than the HSA silica.

The relative intensities of the peaks in the ^{29}Si CP–MAS spectra of the untreated and D_2O-exchanged silicas also provide insight into the differences between external and internal protons. When the CP contact time is 5 ms, the single-silanol peak at –99 ppm has the largest intensity of all peaks in each spectrum of the high $^1H/^2H$ silicas of Figures 3b and 9b as well as the partially proton-bearing silicas of Figures 7b–h and 9e. However, in the spectra of the D_2O-exchanged silicas obtained with the same contact time in Figures 4b′, 4d′, and 6b′, the siloxane peak is the highest in each spectrum. This intensity pattern is consistent with a structural model in which the majority of nearest silicon neighbors of an *external* single-silanol proton is likely to be in single (Q_3) and geminal (Q_2) surface silanols and the nearest silicon neighbors of a trapped, internal single-silanol proton would include a far greater number of siloxane (Q_4) silicons. If these internal silanols were selectively observed by ^{29}Si CP–MAS NMR, the spectrum would manifest the higher proportion of neighboring siloxanes in terms of a correspondingly large Q_4 peak. Likewise, for a silica dominated by external silanols, a ^{29}Si CP–MAS spectrum obtained with a relatively small CP contact time should exhibit more single-silanol intensity than siloxane intensity. The experimentally-observed intensities of both internal and external silanols obtained with a 5-ms contact time (*vide supra*) consistently support this kind of structural model.

The most striking distinction between the ^{29}Si CP–MAS spectra of silicas with external protons in normal isotopic abundance and those subjected to D_2O exchange is the virtual absence of a geminal-silanol peak in the spectra of the D_2O-exchange silicas. However, even a small degree of reprotonation (via marginally effective exchange with gaseous ^1H_2O that is depicted in the spectrum of Figure 8b) reintroduces significant geminal-silanol intensity. Hence, it is clear that most of the geminal silanols are surface accessible by water. In addition to providing useful information about the properties of internal and external silanols, the presence or absence of a geminal-silanol peak permits us to assess the quality of the D_2O-exchange process. If the ^{29}Si CP–MAS spectrum shows strong evidence of a geminal-silanol peak, we know that a substantial number of exterior protons remain unexchanged.

Another observed feature that distinguishes between exterior and interior protons is the difference in spin–lattice relaxation properties of the two environments. A small, apparent T_1^H increase was observed in going from the LSA silica (0.26 s) to the somewhat drier LSA-^1H-25 silica (0.30 s). The exterior protons of the partially reprotonated LSA-*d*-25 and HSA-95*d*-25 silicas (those that are generated by partial reprotonation) exhibit a spin–lattice relaxation time of 0.91 s. However, the internal protons of these and other D_2O-exchanged samples (the residual protons after D_2O exchange) have a quite different T_1^H value, 6.8 s (see Table I). The presence of two distinct T_1^H values for the protons in both the partially reprotonated HSA-95*d*-25 silica and the LSA-*d*-25 silica that was exposed to air for 90 s indicates that ^1H spin exchange between these two spin reservoirs is very inefficient. This lack of spin exchange is evidence that two distinct types of protons exist—the internal protons and the external protons.

After establishing that signals in the ^{29}Si CP–MAS NMR spectra of various D_2O-exchanged samples arise from sources inside the silica particles, we turn our attention to the spin dynamics of the –99 ppm peak in the ^{29}Si CP–MAS NMR spectra in such samples. Table I indicates that the T_{Si-H} value of the –99 ppm resonance arising from internal single silanols (samples HSA-*d*-25, LSA-*d*-25, and LSA-*d*-100) is roughly 12 ms, in contrast to 2.5 ms for the –99 ppm signal attributed to single silanols on the surface (samples HSA, LSA, and LSA-^1H-25). This large T_{Si-H} value for internal single silanols indicates that the relevant $^1H-^{29}Si$ dipolar interactions are much weaker for internal single silanols than those for single silanols on the surface.

Additional evidence that supports the idea that the $^1H-^{29}Si$ dipolar interactions of internal single silanols are weaker than those of surface single silanols is provided by ^{29}Si CP–MAS experiments in which the ^1H decoupling power is varied sys-

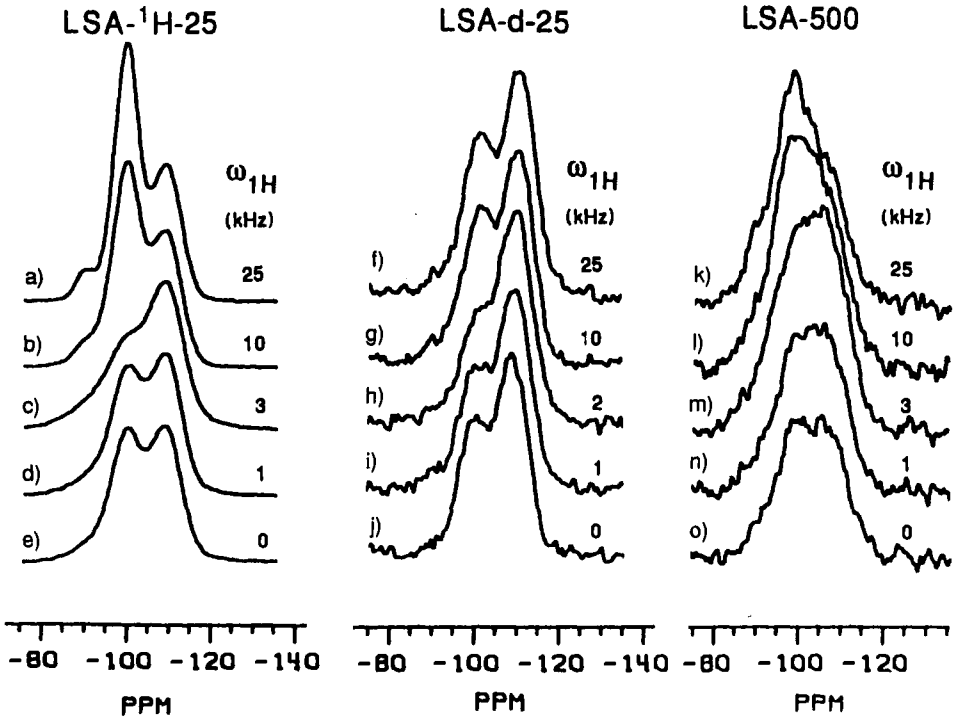

Figure 10. 39.75-MHz ^{29}Si CP–MAS NMR spectra of LSA-^{1}H-25 (a–e), LSA-*d*-25 (f–j), and LSA-500 (k–o) obtained at the various ^{1}H-decoupling fields shown. MAS speed = 1.6 kHz; contact time = 5 ms. Repetition delay: LSA-^{1}H-25, 1 s; LSA-*d*-25, 3 s; and LSA-500, 20 s. Number of acquisitions: LSA-^{1}H-25, 1000; LSA-*d*-25, 4000; and LSA-500, 800. Spectra of a given sample are all plotted on the same intensity scale.

tematically. Figures 10a–j show ^{29}Si CP–MAS NMR spectra of LSA-^{1}H-25 and LSA-*d*-25 silicas obtained with various ^{1}H-decoupling power levels. The top spectrum of each set was obtained with full ^{1}H decoupling (25 kHz in this large-volume MAS system), while the bottom spectrum of each set was acquired without any ^{1}H decoupling. Under magic-angle spinning conditions, if a given proton does not alter its spin state during a rotor period (t_r) and if motion of the ^{1}H–^{29}Si internuclear vector is in either a slow limit or a fast limit (relative to the MAS speed), then the ^{29}Si NMR signal observed after successive rotor periods (nt_r) will not be broadened by ^{1}H–^{29}Si dipolar interactions *in the absence of ^{1}H decoupling*; under these circumstances, magic-angle spinning is sufficient to refocus the inhomogeneous ^{1}H–^{29}Si dipolar interaction after every rotor period. On the other hand, if the ^{1}H spin state changes through ^{1}H–^{1}H spin flip-flops and/or if chemical exchange and/or motion of the ^{1}H–^{29}Si internuclear vector occurs in the intermediate rate regime (comparable to the MAS speed), then the ^{29}Si magnetization signal can not be refocused completely by MAS and the extent of the resulting broadening reflects the combined effect of these changes and the strength of ^{1}H–^{29}Si dipolar interactions. Qualitatively, for a given degree of modulation of the ^{1}H–^{29}Si dipolar interaction in the intermediate frequency regime, stronger ^{1}H–^{29}Si dipolar interactions will result in greater broadening of the ^{29}Si NMR signal in ^{1}H-coupled spectra. Of course, if there are no ^{1}H–^{29}Si dipolar interactions, the ^{29}Si NMR signal will not be affected by turning off the ^{1}H decoupler.

In the spectra of each sample shown in Figure 10, the peak height of the single-silanol resonance at –99 ppm passes through a minimum when $\omega_{1H} \sim$ 1–3 kHz. This decrease in peak height appears to be correlated with an increased line width for the peak. As the ^{1}H decoupling power is increased from zero, broadening of the single-silanol ^{29}Si peak is maximized (at $\omega_{1H} \sim$ 1–3 kHz) before the power reaches sufficient levels to decouple the ^{1}H spins effectively. In order to study this broadening in more detail, the spectrum with the lowest single-silanol peak height (and presumably the maximum line width) for each sample was deconvoluted into the Q_2, Q_3, and Q_4 peaks that comprise these overlapping spectra. The fully decoupled spectrum for each sample was also deconvoluted. Typical deconvolution results are shown in Figure 11. The deconvolution results indicate that the maximum increase in line width achieved by varying ω_{1H} is larger for the external single silanols of LSA-^{1}H-25 silica than for the internal single silanols of LSA-*d*-25 silica. At least two substantially related phenomena could be responsible for the existence of broadening maxima observed in the ω_{1H} variation displayed in Figure 10.

According to one view, *any* time dependence of the ^{1}H–^{29}Si dipolar interaction (due to flip-flops, chemical exchange, or motion) on a time scale comparable to t_r will interfere with the MAS averaging of the ^{1}H–^{29}Si dipolar interaction, leading to a broadening. It is difficult to predict how a complicated array of such time-dependent phenomena might behave overall, vis-à-vis of the dependence of line width on ω_{1H}. It would not be surprising if the interplay of line-broadening effects maximized for some finite, nonzero value of ω_{1H}, but it does not seem realistic to extract quantitative information on the strength of ^{29}Si–^{1}H dipolar interactions from the detailed ω_{1H} dependence of the spectra of Figure 10.

The second type of phenomenon that could account for the trends seen in Figure 10 is rotary resonance recoupling,[66,67] to which the variable-decoupling experiments represented in Figure 10 also bear a resemblance. This phenomenon involves isolated I–S spin pairs in which the spectrum of the S spin is observed while the I spins are coherently nutated at a frequency (ω_{11}) that is a small-integer multiple of the MAS frequency (ω_r). Under these conditions, the heteronuclear interaction is "recoupled"; thus, the isotropic peak and any shielding anisotropy sidebands of the S spin are broadened. The broadening observed in rotary resonance recoupling also reflects the strength of the effective I–S dipolar interaction. In contrast to typical rotary resonance recoupling, the variable-decoupling experiments reported here may not employ sufficient ^{1}H-decoupling power in the regime of maximum broadening for coherent ^{1}H nutation that would overcome the strong homonuclear dipolar interactions present

(66) Oas, T. G.; Griffin, R. G.; Levitt, M. H. *J. Chem. Phys.* **1988**, *89*, 692.
(67) Levitt, M. H.; Oas, T. G.; Griffin, R. G. *Isr. J. Chem.* **1988**, *28*, 271.

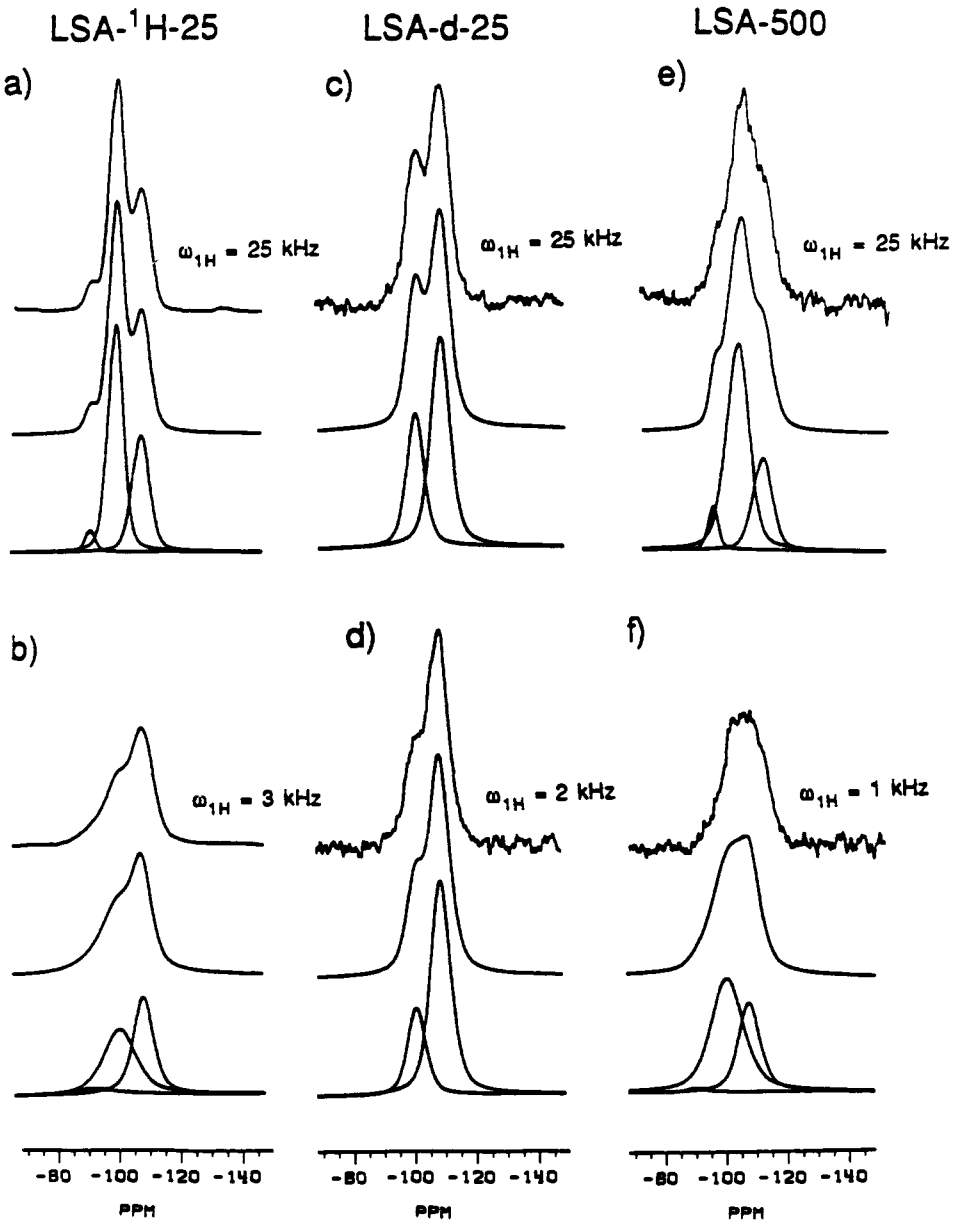

Figure 11. Deconvolutions of selected spectra from Figure 10. Each set of spectra includes the experimental spectrum (top), a simulated spectrum (middle), and the deconvoluted contributions (bottom) to the simulated spectrum: (a) LSA-^{1}H-25, ω_{1H} = 25 kHz; (b) LSA-^{1}H-25, ω_{1H} = 3 kHz; (c) LSA-*d*-25, ω_{1H} = 25 kHz; (d) LSA-*d*-25, ω_{1H} = 2 kHz; (e) LSA-500, ω_{1H} = 25 kHz; and (f) LSA-500, ω_{1H} = 1 kHz.

among the populations of protons on silica. In any case, the LSA-^{1}H-25 and LSA-*d*-25 spectra in Figure 10 with maximum single-silanol broadening occur at $\omega_{1H} \approx \omega_r$ or $2\omega_r$. Variable-decoupling experiments performed on external silanols at various MAS spinning speeds (not shown here) indicate that the decoupling field strength with maximum broadening (ω_{1max}) increases along with the MAS frequency over the 0.8–2.5-kHz range studied.

Irrespective of the mechanism that undermines MAS averaging of the ^{1}H–^{29}Si dipolar interaction in the variable-decoupling experiments, one can note that there are marked differences in the behavior of the single-silanol peaks of the LSA-^{1}H-25 and LSA-*d*-25 silicas in these experiments. The line widths and areas of the deconvoluted peaks from Figure 11 are compiled in Table II. In both the LSA-^{1}H-25 and LSA-*d*-25 samples, the single-silanol Q_3 peak loses roughly one-third of its fully decoupled peak area in the spectrum with maximum Q_3 broadening. This loss of intensity can be attributed to silanol populations found in both external and internal environments that experience very strong ^{1}H–^{29}Si dipolar interactions; the ^{29}Si signals of these silanols are broadened to the extent that they cannot be resolved from baseline noise without the line-narrowing provided by high-power ^{1}H decoupling.

The remaining portion (two-thirds) of the ^{29}Si signals exhibits differing behavior in external and internal environments. The data in Table II indicate that for the predominately external environment of the LSA-^{1}H-25 silica, the Q_3 single-silanol line width more than doubles from 275 Hz with full decoupling to 593 Hz in the maximally broadened spectrum. However, the internal single silanols of the LSA-*d*-25 silica maintain nearly the same line width of just over 300 Hz in both spectra. The broadening in the maximally broadened spectrum of the external silanols (LSA-^{1}H-25) is indicative of a stronger ^{1}H–^{29}Si dipolar interaction than that seen for the majority of internal silanols (LSA-*d*-25) that exhibit virtually no broadening in the spectrum.

The cross-polarization time constants for LSA-^{1}H-25 and LSA-*d*-25 can also provide an indication of the different magnitudes of the ^{1}H–^{29}Si dipolar interactions. The CP time constant is roughly a measure of the inverse of the square of the magnitude

Table II. Parameters Derived for Deconvoluted Peaks of ^{29}Si CP–MAS Spectra of Various Silicas

sample	ω_{1H} (kHz)	peak	LW_{HM} (Hz)[a]	peak area (Arbs.)
LSA-^{1}H-25	25	Q_2	194	114
		Q_3	275	1676
		Q_4	319	999
LSA-^{1}H-25	3	Q_2	738	132
		Q_3	593	1146
		Q_4	361	1040
LSA-*d*-25	25	Q_3	314	951
		Q_4	350	1668
LSA-*d*-25	2	Q_3	332	633
		Q_4	366	1706
LSA-500	25	Q_2	182	214
		Q_3	416	2323
		Q_4	360	898
	1	Q_2	292	37
		Q_3	593	1989
		Q_4	395	1037

[a] Line width at half maximum.

of the ^{1}H–^{29}Si dipolar interaction.[68] We have shown that T_{Si-H} for internal single silanols is roughly 4.5–5.0 times larger than T_{Si-H} for external single silanols. This implies that the external single silanols experience ^{1}H–^{29}Si dipolar interactions that are slightly more than twice as strong as those seen for internal single silanols.

Several factors, structural and dynamical, could account, in principle, for this apparent difference in the strengths of the ^{1}H–^{29}Si dipolar interactions in the LSA-^{1}H-25 and LSA-*d*-25 samples. The most obvious factor would be a difference in the ^{1}H–^{29}Si internuclear distance for the single silanols in internal and external environments. In both cases, the two relevant nuclei are "connected" via a bridging oxygen, a situation that imposes substantial constraints on the structures that can be expected to exist. The chemical similarities of these systems impose severe requirements on variations in bond lengths and angles, despite differences in their physical environments. Nevertheless, variations of the Si–O–H bond angle could lead to some variation in Si–O–H internuclear distances. A reduction of the Si–O–H angle from, say 108° to 95° would lead to a reduction of the Si–O–H distance from about 2.10 Å to about 1.95 Å, which would account for a factor of about 5 in T_{Si-H}. Alternatively, it is possible that the Si–O–H angle in internal silanols may be substantially larger than 109°, leading to larger Si–O–H distances and correspondingly larger T_{Si-H} values. However, motional dynamics may also be responsible for the difference in T_{Si-H} values.

Peri[24] found evidence for rotation or torsional oscillation about the Si–OH bond of dried silica and obtained a Si–O–H bond angle of 113° for external Si–OH groups. The IR band at 3660 cm^{-1} has been assigned to internal silanols by many workers.[6,33-40,43] While IR adsorption between 3400 and 3500 cm^{-1} is assigned to *strongly* hydrogen-bonded OH groups,[45] Peri[24] and McDonald[45] attributed the 3660-cm^{-1} band to *weakly* H-bonded OH groups. *A priori*, it is possible that the hydroxyl groups of internal single silanols, unlike many of the external silanols, experience only weak (at most) hydrogen bonding and rotate around the Si–OH axis rapidly enough to partially average the ^{1}H–^{29}Si dipolar interaction. If one assumes the same bond angle of 113° for internal Si–OH as Peri calculated for external Si–OH and uses "typical" bond lengths of 0.097 nm for O–H[24] and 0.163 nm for Si–O,[69] then one determines that the ^{1}H–^{29}Si internuclear vector rotates at an angle of 24° relative to the ^{1}H–^{29}Si rotational axis (which is coincident with the Si–O bond axis), as shown in Figure 12a. For a rapid rotation, the ^{1}H–^{29}Si dipolar interaction within a given SiOH moiety would thereby be scaled down[70] by the

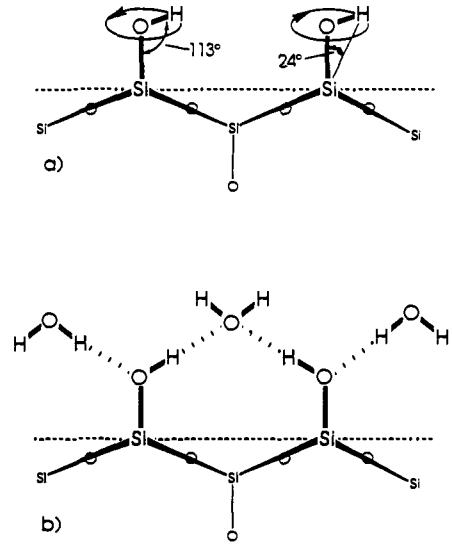

Figure 12. Proposed silanol structure and interactions for (a) rotating single silanols and (b) rigid, hydrogen-bonded single silanols.

factor $^1/_2(3\cos^2 24° - 1) = 0.75$. On the surfaces of untreated silica gels, hydroxyl rotation of single silanols may be hindered or held rigid through strong hydrogen bonding with water,[51,71] as shown in Figure 12b. In contrast to the rotating internal silanols postulated above, the more rigid single silanols on the surface of an untreated silica would experience a larger, less rotationally-averaged ^{1}H–^{29}Si dipolar interaction.

Yet another factor should also contribute to the ratio of dipolar interactions seen for external and internal silanols. If the external single silanols are rigidly hydrogen-bonded to water and other neighboring silanols, then the protons of these nearby species also contribute to the ^{1}H–^{29}Si dipolar interaction of the silicons of external single silanols. The majority of internal silanols would have no contributions from additional protons because they do not participate in hydrogen bonding. Hence, hydrogen bonding can be expected to increase the strength of the ^{1}H–^{29}Si dipolar interaction of the external single silanols relative to that of the internal silanols by two mechanisms; it increases the number of protons that interact with each silanol silicon, and it restrains motional averaging of the dipolar interactions.

If hydrogen bonding is the true cause of this larger dipolar interaction in external silanols, then removal of the hydrogen bonding of the external silanols should result in similar behavior to that observed for internal silanols. Evacuation at 500 °C is known to eliminate all water and virtually all hydrogen-bonded silanols from an external silica surface. A sample (LSA-500) was prepared in this manner, and the variable-decoupling experiment was performed on it; the results are shown in Figures 10k–o. After evacuation at such a high temperature, the Q_2, Q_3, and Q_4 peaks in the ^{29}Si NMR spectra of silica gels are known to broaden substantially,[72] and the spectrum of LSA-500 in Figure 10k clearly demonstrates this broadening, which is attributed to the introduction of a distribution of structures on the silica surface due to the formation of strained Si–O–Si moieties. The wider variety of Q_2, Q_3, and Q_4 structures produced by high-temperature treatment results in a wider distribution of chemical shifts for each of these surface species and in broader peaks, which make deconvolutions more difficult. When the additional broadening due to recoupling the ^{1}H–^{29}Si dipolar interaction is introduced via ω_{1H} variation, the deconvolutions become even more problematical. Nevertheless, the deconvolution shown in Figure 11e for the *decoupled* spectrum of LSA-500 is the only combination of peak intensities and line widths that accurately simulates the experimental spectrum. However, the deconvolution of the

(68) Slichter, C. P. *Principles of Magnetic Resonance*, 3rd ed.; Springer-Verlag: New York, 1989; p 79.
(69) Wells, A. F. *Structural Inorganic Chemistry*, 5th ed.; Clarendon Press: Oxford, U.K., 1984; p 1000.
(70) Gutowsky, H. S.; Pake, G. E. *J. Chem. Phys.* **1950**, *18*, 162.
(71) Kiselev, A. V.; Lygin, V. I. *Kolloidn. Zh.* **1959**, *21*, 581.
(72) Sindorf, D. W.; Maciel, G. E. *J. Am. Chem. Soc.* **1983**, *105*, 1487.

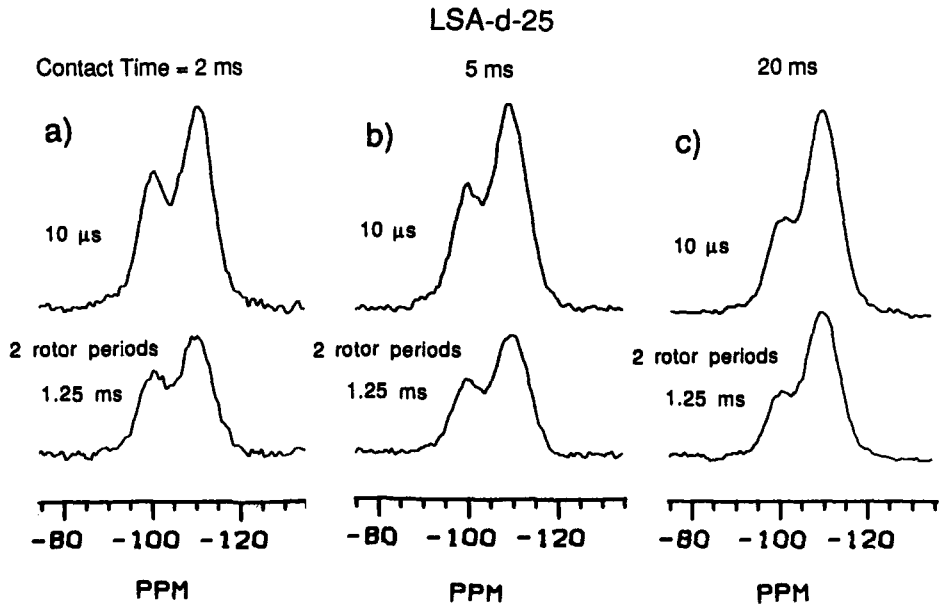

Figure 13. 39.75-MHz ^{29}Si CP–MAS NMR spectra of LSA-*d*-25 with 10-μs (top spectrum of each set) and 2 rotor period (1.25 ms, bottom spectrum of each set) of ^1H–^1H dipolar dephasing prior to $^1H \rightarrow {}^{29}Si$ cross polarization, with three different CP contact times: (a) 2 ms, (b) 5 ms, and (c) 20 ms. Spectra within each set are plotted on the same intensity scale.

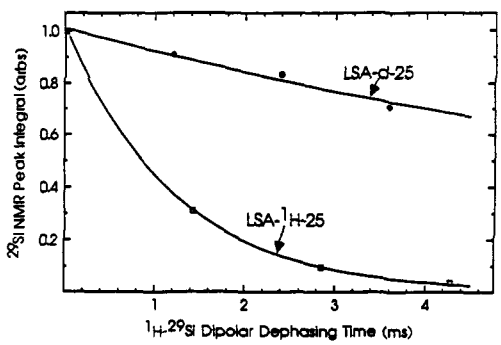

Figure 14. Plots of single-silanol ^{29}Si CP–MAS peak integrals obtained after ^1H–^{29}Si dipolar-dephasing times corresponding to even-integer multiples of the MAS rotor period. Integrals are normalized so that the first data point for each sample (dephasing time = 20 μs) has a peak integral of unity. CP contact time = 5 ms: (□) LSA-^{1}H-25, repetition delay = 1 s, MAS speed = 1.4 kHz and (•) LSA-*d*-25, repetition delay = 6 s, MAS speed = 1.6 kHz.

recoupled spectrum of this sample in Figure 11f is only one of several combinations of peak intensities and line widths that could simulate the experimental spectrum. Selecting the "correct" deconvolution is a subjective process. The particular deconvolution shown in Figure 11f represents the combination of peaks that permits the single-silanol (Q_3) peak to have the largest possible line width that would make it possible to simulate the experimental spectrum satisfactorily. Other, equally acceptable deconvolutions were composed of narrower Q_3 peaks and larger, narrower Q_2 peaks than those shown in Figure 11f. However, even with this broadest estimate of the maximal (recoupled) Q_3 line width of LSA-500 that is shown in Figure 11f and tabulated in Table II, the recoupled line width is only about 42% larger than the decoupled Q_3 line width seen in Figure 11e. This variable-decoupling broadening of the Q_3 line width for the LSA-500 silica is far less than the roughly 215% increase in line width seen for the rigid external silanols of the LSA-^{1}H-25 silica. The fact that these unbound, ostensibly freely rotating, external silanols of the LSA-500 silica exhibit behavior that is qualitatively similar to that of the internal silanols (LDA-*d*-25) supports the model of unbound, freely rotating, internal silanols.

In order to explore the nature of the internal single silanols in more detail, a previously described,[21] rotor-synchronized, ^1H–^1H dipolar-dephasing experiment was employed. In this experiment, ^1H magnetization is allowed to dephase in the transverse plane for two rotor periods. A π pulse is applied to the protons at the end of the first rotor period of dephasing. With ^{29}Si dipolar decoupling in effect during this dephasing period, all inhomogeneously behaving ^1H–^1H dipolar interactions are refocused at the end of two rotor periods. Homogeneous interactions such as ^1H–^1H spin exchange give rise to an attenuation in the ^{29}Si signals observed when this dephasing period is inserted into the CP–MAS experiment.

Figures 13a–c show spectra of LSA-*d*-25 silica obtained using ^1H–^1H dipolar-dephasing periods of 10 μs (considered here to be essentially the absence of a dephasing period) and two rotor periods (1.25 ms) prior to three different CP contact times. Figures 13a and 13b indicate that 40% of the CP–MAS ^{29}Si NMR signal intensity from internal single silanols (–99 ppm) and siloxanes (–109 ppm) disappears after two rotor periods of ^1H–^1H dipolar dephasing prior to a 2- or 5-ms cross-polarization contact period. The ^1H magnetization sources responsible for both ^{29}Si peaks dephase at the same rate; and the dephased ^1H polarization is not significantly depleted nor repolarized through spin exchange with other ^1H spin reservoirs as the CP contact time is increased from 2 to 5 ms. This implies that the –99 and the –109 ppm peaks may have the same ^1H source (single silanols) for cross polarization and that these single silanols are isolated from other ^1H spin reservoirs on a time scale of at least 5 ms. Figure 13c indicates that, during the 20-ms CP contact period, protons of internal single silanols recover 15% of their initial dephased intensity from some *other* ^1H spin reservoir. The *only* other protons *in* the silica would be from internal or "trapped" water. This result indicates that at least some small fraction of the internal single silanols may be accompanied by trapped water.

In a previous study[21] of untreated silica gel, it was found that the –99 ppm peak lost 91% of its intensity after two rotor periods of ^1H–^1H dipolar dephasing prior to cross polarization with contact times of 0.1, 0.3, 1, and 5 ms. Obviously, dephasing of the ^1H spin polarization of the single silanols on the untreated silica *surface* (the majority of silanols of untreated silica gel) is much faster than that of *internal* single silanols, reflecting a substantial difference in the strengths of ^1H–^1H dipolar interactions of these two types of silanols. If single silanols on the surface are in a hydrogen-bonded network with water molecules, as depicted in

Figure 12b, then their ^1H–^1H dipolar interaction would be expected to be much stronger than those of internal single silanols.

The combined effects of ^1H–^1H and ^1H–^{29}Si dipolar interactions can be investigated by monitoring the decay of ^{29}Si CP–MAS NMR intensities acquired following ^1H–^{29}Si dipolar-dephasing times that correspond to even-integer multiples of the MAS rotor period of a previously described experiment.[21] Even multiples of the rotor period are employed as dephasing times ($2nt_r$) to eliminate any dephasing by inhomogeneous behavior of the dipolar interactions and the chemical shift anisotropy. For a given extent of ^1H–^1H flip-flops (^1H dipolar dephasing), the decay rate of ^{29}Si NMR intensity in this experiment will be faster for a stronger ^1H–^{29}Si dipolar interaction. On the other hand, for a given ^1H–^{29}Si dipolar pair, a faster ^1H–^1H flip-flop rate will cause a faster decay of ^{29}Si NMR intensity. As seen in Figure 14, the –99 ppm peak (internal single silanols) in the ^{29}Si CP–MAS NMR of LSA-*d*-25 has a dephasing time constant of 11.0 ms in the ^1H–^{29}Si dipolar-dephasing experiment (monitored at dephasing times of even multiples of the rotor periods), about 9 times larger than the 1.2 ms seen in Figure 14 for single silanols of the LSA-^1H-25 silica surface. This lengthening of the dephasing time constant is attributed to the combined effects of a weaker ^1H–^{29}Si dipolar pair and a smaller ^1H–^1H dipolar-dephasing rate for internal single silanols than for single silanols on the surface.

Conclusions

^{29}Si CP–MAS NMR studies of D_2O-exchanged silica gels indicate that there are very few, if any, geminal silanols present inside silica gel particles. Of the single silanols present in an unexchanged sample of a lower surface-area silica gel, 9.3% could not undergo D_2O-exchange at 25 °C, and these unexchangeable single silanols are believed to be located "inside" the silica gel particles. The amount of internal single silanols unavailable for D_2O exchange is reduced to 4.0% when the D_2O exchange is performed at 100 °C. Only 3.0% of the initial single silanols in a higher surface-area silica gel remains after D_2O exchange at 25 °C.

On the basis of the large T_{Si-H} values and the results from experiments in which the ^1H-decoupling power was varied, we conclude that the hydroxyl groups of internal single silanols may rotate rapidly about the Si–OH bond axis, reducing the ^1H–^{29}Si dipolar interaction substantially. Experiments with ^1H–^1H dipolar dephasing prior to $^1H \rightarrow {}^{29}Si$ cross polarization and experiments with ^1H–^{29}Si dipolar dephasing also provide evidence for a rotating hydroxyl group of internal single silanols and indicate that at least some of the internal single silanols have trapped water accompanying them.

Acknowledgment. The authors gratefully acknowledge support of this research by National Science Foundation Grant No. CHE-9021003.